ELSEVIER

Journal of Nuclear Materials 241–243 (1997) 919–924

journal of nuclear materials

Section 5. Other devices

Mass spectroscopic measurements in the plasma edge of the W7-AS stellarator and their statistical analysis

P. Zebisch *, P. Grigull, V. Dose, E. Taglauer, W7-AS Team

Max-Planck-Institut für Plasmaphysik, EURATOM-Association, D-85748 Garching bei München, Germany

Abstract

During the W7-AS operation period in autumn 1995 sniffer probe measurements were made for more than 800 discharges. The H/D ratio during deuterium discharges was determined showing HD and H_2 desorption from the walls even after fresh boronization. For these discharges the loading of the walls with deuterium could be observed. In the higher mass range the development of large amounts of hydrocarbons was observed at the beginning of the discharges with neutral beam injection. To evaluate the large amount of data recorded here (order of 10000 mass spectra), appropriate mathematical methods are required. It is shown that group analysis can be applied to distinguish certain sets of discharges and to derive useful mean values.

Keywords: W7-AS; Impurity source; Wall pumping; Mass spectrometry

1. Introduction

Mass spectroscopy can be a useful diagnostic tool in fusion devices for the investigation of various physical aspects, e.g. to monitor the effects of wall conditioning and plasma–wall interaction [1], to investigate isotope effects on plasma confinement [2,3] or to monitor the isotope ratio for minority heating with ICRH (ion cyclotron resonance heating) [4].

Mass spectroscopic measurements with so called sniffer probes have been done in several fusion devices [5–8]. Here we report on measurements at the Wendelstein W7-AS stellarator, a modular advanced stellarator with a major radius $R = 2$ m, an effective plasma radius of about 0.2 m and fivefold symmetry [9,10].

The sniffer probe for the experiments of this work has been used before in the ASDEX tokamak [5] as well as in the W7-AS stellarator [6]. The graphite head on top of a tube has an opening with 8 mm in diameter that determines the position for gas detection. It is equipped with three Langmuir probes that were only used to determine the position of the probe relative to the plasma. The neutral gas and the neutralized ion flux are detected at the end of a tube of about 2 m length by a Balzers QMG 511 quadrupole mass spectrometer that is differentially pumped. The whole setup has a time constant of less than 100 ms for hydrogen and deuterium.

The sniffer probe is mounted at the port 8 in Section 3 of W7-AS where the shape of the plasma is nearly elliptical with the longer axis slightly tilted away from the vertical. This port is not centered below the ellipse so that the probe hits the outer side of the plasma.

In the operation period in autumn 1995 spectra from more than 800 discharges were taken. During one discharge the mass range of interest is repeatedly scanned with a maximum scan speed of 10 ms/u which means that every 40 ms a spectrum in the range $m/e = 1$ to 4 can be taken which was done for about 600 discharges. The repetition rate for the 200 spectra over a larger mass range is consequently lower.

2. Measurements in the range $m/e = 1$ to 4

2.1. H/D ratio

In this section we present results concerning the development of the hydrogen and deuterium content during

* Corresponding author. Tel.: +49-89 3299 1757; fax: +49-89 3299 1149; e-mail: ptz@ipp-garching.mpg.de.

PII S0022-3115(96)00632-0

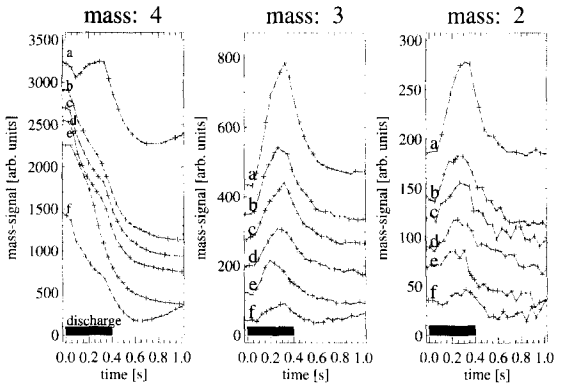

Fig. 1. Time behavior of $m/e = 1$ to 4 for ICRH test discharges at various z-positions of probe. z-positions in cm below middle plane: (a) 22.5 ($r_{eff} = 22.3$), (b) 24.5, (c) 25.5, (d) 28.5, (e) 30.5, (f) 35.5. The zero-lines for consecutive spectra are shifted.

discharges that were made for ICRH test purposes. For these discharges a low H/D ratio is important for the efficiency of ICRH minority heating. Fig. 1 shows the signals for the masses 2 to 4 for various z-positions (distance below horizontal middle plane of W7-AS) of the sniffer probe in similar discharges. The opening of the sniffer head was oriented perpendicular to the magnetic field which results in ion flux and neutral gas detection for small and in only neutral gas detection for large z-positions. Outside the plasma, for large z-positions, a decline of the $m/e = 4$ signal with time is observed due to the pumping of the plasma. For the lowest z-position ($r_{eff} =$ 22.3 cm, curve a) an increase can be observed that shows the enlarged particle flow to the probe in the scrape off layer of the plasma. This signal also decreases at the end of the discharge at about 0.4 s with the decay time of the vacuum vessel (less than 130 ms). The $m/e = 3$ signal shows a completely different behavior. It increases for all

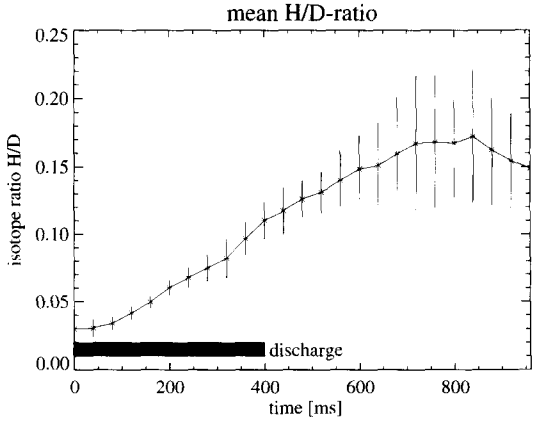

Fig. 2. Mean H/D ratio at $z = 35.5$ cm for the similar discharges #34330–#34353. Similarity is guaranteed by group analysis.

z-positions, but most for the smallest z-position. This shows that there must be hydrogen in the vessel although only deuterium is puffed in. This hydrogen originates from the walls and reacts with deuterium ions or atoms formed in the discharge to build up HD that desorbs from the walls. This effect also occurs at the surfaces of the probe and therefore the signal is highest close to the plasma (position a) where the H- and D-ion fluxes are highest. The $m/e = 2$ signal in principle shows the same behavior as the $m/e = 3$ signal, but the overall signal is smaller because of the smaller probability for H_2 formation compared to HD formation. From that behavior it can also be concluded that the $m/e = 2$ signal from cracked D_2 is small, as expected from the D_2 cracking pattern (mass 4/mass 2 ≈ 50).

From these measurements together with the measured sensitivities for H_2 and D_2 and the interpolated sensitivity for HD the H/D isotope ratio for each discharge can be determined, which will be presented in a forthcoming paper. The interpolation is justified by the rather small variation in sensitivity (factor 1.3) between $m/e = 2$ and $m/e = 4$. In this work a mean value, averaged over 23 discharges, for the isotope ratio with time for ICRH test discharges at a distance of $z = 35.5$ cm, i.e. outside the plasma edge, is presented in Fig. 2. The similarity of the discharges out of the series #34330 to #34353 that were selected for the mean value formation was guaranteed by group analysis. The series was made directly after boronization with deuterated diborane. In this measurement the increase in H/D ratio during but also after the discharge is clearly visible, starting with a value of 0.03 and peaking at about 0.18 after 800 ms which means about 400 ms after the end of the discharge. This demonstrates

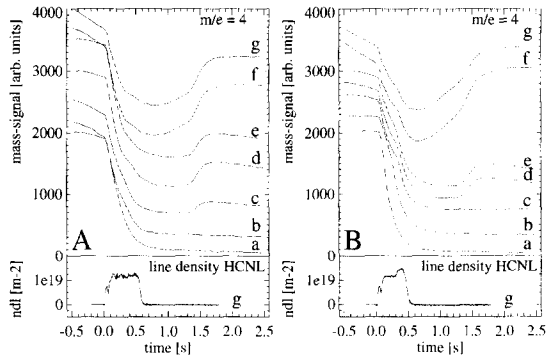

Fig. 3. First discharges of experiment day. A: ICRH test discharges directly after boronization (a) # 34331, (b) #34332, (c) #34333, (d) #34335, (e) #34336, (f) #34337 (g) #34338. B: ICRH test discharges on the second day after boronization (a) #33902, (b) #33903, (c) #33904 (d) #33905, (e) #33906, (f) #33909, (g) #33911. The zero-lines for consecutive spectra are shifted. For spectrum (g) the time development of the line density is depicted.

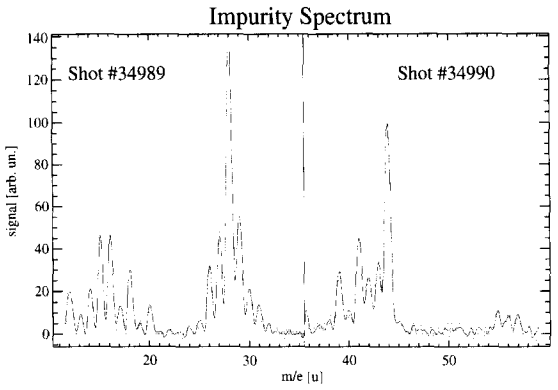

Fig. 4. Typical impurity spectrum at the beginning of an NBI heated discharge.

that the rate of hydrogen release from the wall is determined by diffusion and desorption processes, that are both necessary for hydrogen release, on a time scale larger than the discharge time. The present measurements do not allow to determine the rate limiting step.

2.2. Deuterium loading of the wall

Another interesting feature observed in the ICRH test discharges is the loading of the walls with deuterium. The evolution with time for $m/e = 4$ of the first discharges of the day, all starting with an initial pressure of about 10^{-3} mbar, is depicted in Fig. 3. The development of the signal for the initial discharges (curves a–b in Fig. 3A and a–c in Fig. 3B) is different from the others although in all discharges the plasma density is kept at the same constant value by the gas inlet. These curves do not show any increase of the $m/e = 4$ signal at about 1.3 s (0.9 s after the end of the discharge) which is observed in later discharges and finally saturates after about 7 to 8 discharges.

The series in Fig. 3B was taken on the second experiment day after boronization with deuterated diborane, whereas the series in Fig. 3A was taken directly after boronization. There is obviously no difference in the behavior of the two sets which leads to the result that the wall surfaces contain hydrogen also after this kind of boronization. This also means that the walls slowly gas out deuterium during the standing periods between experiment days, whereas the time between the discharges is not long enough to get rid of the gas on and in the walls. Helium glow discharges are made several times during operation days, but this appears not to influence the measurements presented here.

3. Impurity production at the beginning of NBI

One of the most prominent features detected in the spectra outside the mass range $m/e = 1$ to 4 is the rather

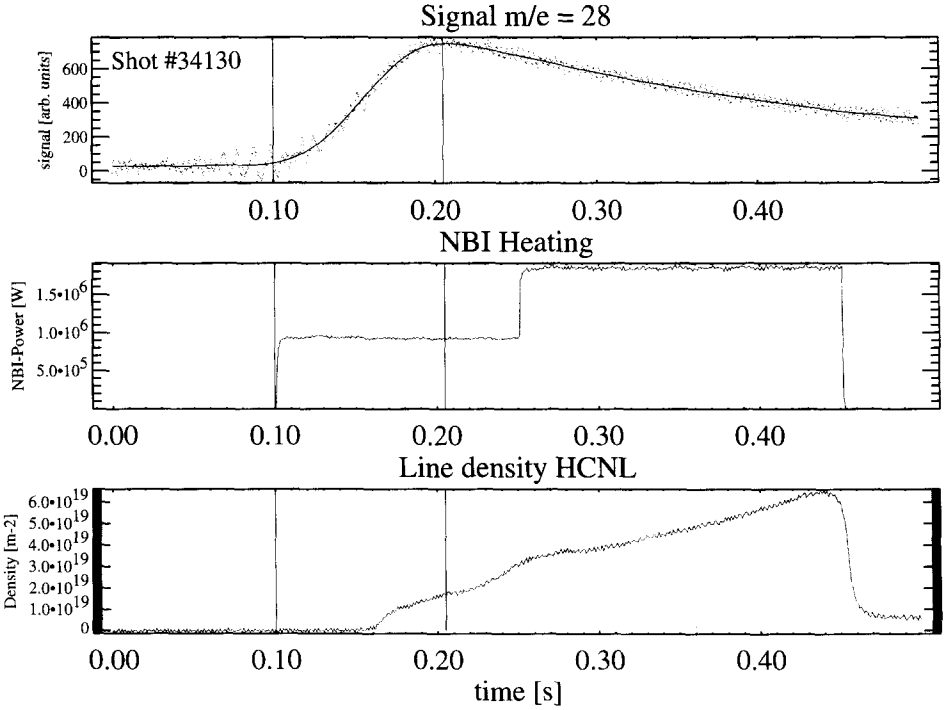

Fig. 5. $m/e = 28$ signal versus time in correlation with NBI-power and line density. First vertical line indicates NBI-onset, second vertical line maximum of impurity signal. Plasma formation is with the help of an hf-pulse (900 MHz).

large signal (up to 10% of $m/e = 2$ signal) for hydrocarbons during most of the discharges with neutral beam injection (NBI) heating, whereas in other discharges no impurities can be detected. A typical spectrum for the detected impurities at $t \approx 300$ ms is depicted in Fig. 4 that is composed from measurements of two different discharges. Visible is a spectrum typical for hydrocarbon production with the largest peaks at $m/e = 28$ and $m/e = 44$ which are also due to CO and CO_2, respectively.

In Fig. 5 the development of the $m/e = 28$ signal with time for a discharge with NBI heating is displayed together with the NBI-power and the line density measured with the HCN-laser. The position of the sniffer probe was at $z = 45.5$ cm which means in the tube of the port to which it is mounted. This ensures that the hydrocarbons are not produced in a reaction of the plasma or the neutral beam with the graphite head. The first vertical line shows that the $m/e = 28$ signal starts to increase with the onset of NBI. It continues growing, peaks at about 200 ms and slowly decreases again for later times and increasing line density.

The observed effect can be explained by looking at the geometry of the W7-AS stellarator, the position of the sniffer probe and the orientation of the neutral beams. This leads to the following scenario: The discharge is started by the 900 MHz preionization leading to a very thin plasma whose line density cannot be detected by the HCN-laser. The NB is injected into this thin plasma, part of it traversing it and hitting the wall about 20 cm away from the sniffer probe. Apart from heating the walls which leads to impurity desorption, reactions between the hydrogen atoms and graphite parts of the wall lead to an efficient production of hydrocarbons. In the further course of the discharge the plasma gets denser and a smaller and smaller part of the NB reaches the wall in the neighborhood of the sniffer probe leading to a decrease in the impurity production.

4. Group analysis

Repeated scans over the mass range of interest with a speed of 10 ms/u resulted in more than 40000 single mass spectra. They cannot be analyzed individually, i.e. a method for computer controlled analysis must be found. The way this is done here is the use of group analysis as a statistical method. For this purpose data vectors $\vec{x}$ are formed containing the partial pressures of the masses taken at a certain time t_i as components. The data vectors $\vec{x}$ of different discharges at the same time t_i are put together to represent one group. The analysis of these groups should deliver mean values versus time for the chosen set of discharges. To get sensible results it must be known which discharges may be put together to form one set. Group analysis now delivers a possibility to decide whether the chosen division into sets of discharges is correct or whether the sets must be divided into a greater number of sets.

In the following, the mathematical method will shortly be described. For further details, see e.g. [11].

4.1. Summary of mathematical method

Every spectrum taken at a certain time t_i forms a data vector $\vec{x}_{ij}$ (jth vector in group i). Data vectors of spectra taken at the same time form a group. To get the largest diversion in time look for a direction $\vec{a}$ in which the variation between the groups is 'optimized'.

The $y_{ij} = \vec{x}_{i,j}^{\mathrm{T}}\vec{a}$ are the projections of $\vec{x}_{i,j}$ on $\vec{a}$. 'Optimized' variation between groups means that

$$\Phi = \frac{[1/(g-1)]\sum_{i=1}^{g} n_i(\bar{y}_i - \bar{y})^2}{[1/(n-g)]\sum_{i=1}^{g}\sum_{j=1}^{n_i}(y_{ij} - \bar{y}_i)^2} = \frac{[1/(g-1)]\vec{a}^{\mathrm{T}}\mathbf{B}\vec{a}}{[1/(n-g)]\vec{a}^{\mathrm{T}}\mathbf{W}\vec{a}} \tag{1}$$

has its maximum value with

$$\mathbf{W} = \sum_{i=1}^{g}\sum_{j=1}^{n_i}\left(\vec{x}_{ij} - \bar{\vec{x}}_i\right)\left(\vec{x}_{ij} - \bar{\vec{x}}_i\right)^{\mathrm{T}}, \tag{2}$$

$$\mathbf{B} = \sum_{i=1}^{g} n_i\left(\bar{\vec{x}}_i - \bar{\vec{x}}\right)\left(\bar{\vec{x}}_i - \bar{\vec{x}}\right)^{\mathrm{T}}. \tag{3}$$

$\bar{\vec{x}}_i$ and $\bar{\vec{x}}$ are the means in one group and over all data, respectively. This results in a modified eigenvalue problem:

$$\mathbf{B}\vec{a} - \lambda\mathbf{W}\vec{a} = 0 \tag{4}$$

which leads to a set of eigenvalues and eigenvectors. As can be derived from Eq. (1) the wanted direction $\vec{a}$ is the direction belonging to the eigenvector to the largest eigenvalue.

The different eigenvalues and their corresponding eigenvectors are assigned with λ_m and $\vec{a}_m$. They form a coordinate system and are normalized by $\vec{a}_m^{\mathrm{T}}\mathbf{W}\vec{a}_m = 1$. As

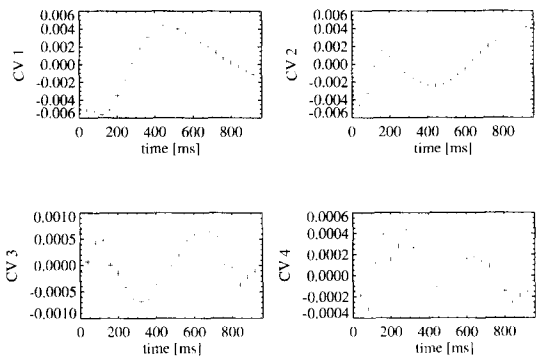

Fig. 6. Time development of canonical variates for all measured data in the range $m/e = 1$ to 4.

a measure of distances in this 'optimized' system the Mahalanobis-distance is gained:

$$d^2_{\vec{y}_{ij}\vec{y}_{kl}} = \left(\vec{x}_{ij} - \vec{x}_{kl}\right)^{\mathrm{T}} \mathbf{W}^{-1} \left(\vec{x}_{ij} - \vec{x}_{kl}\right). \quad (5)$$

A comparison of the distribution of the Mahalanobis distances of the data points to their corresponding group centers with a theoretical distribution that contains only the errors of the measurement shows whether a division into sets of discharges is correct or has to be improved.

4.2. Examples

In a first example the spectra of all 600 discharges in the range $m/e = 1$ to 4 form one set. This leads to four

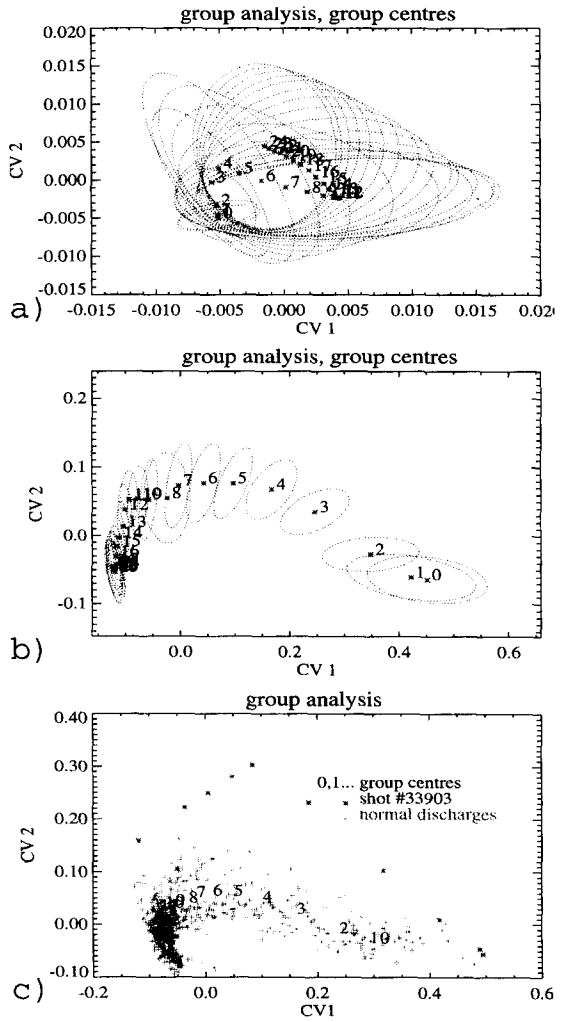

Fig. 7. Representation of data in two canonical variates (CV1 and CV2). Group numbers multiplied by 40 ms give time evolution. (a) Only group centers and standard deviations (ellipses) for all measured data in range $m/e = 1$ to 4, (b) same as (a) for ICRH test discharges that were used for mean H/D ratio in Fig. 2, (c) all data points for same set as (b) plus additional data from another series of same type. The asterisks denote one discharge that does not fit to the others.

eigenvalues, two of which are rather large compared to the other two. The eigenvectors are composed of various contributions of all measured data directions ($m/e = 1$ to 4). The projection of the group centers on all four eigenvectors is depicted in Fig. 6, where the group number is translated into the time at which the spectra were taken. The eigenvectors are assigned with CV1 to 4 (Canonical Variate). It can be seen that only CV1 and CV2 corresponding to the two largest eigenvalues show a time evolution larger than the noise, so that the time development of the spectra is reduced from former 4 directions ($m/e = 1$ to 4) to only two directions that optimize the variation in time.

These two directions form the axes of Fig. 7a where the group centers are depicted again. The numbers give the time evolution shown in Fig. 6 which means that the time for a group can be calculated by multiplying the group number by 40 ms. The ellipses in Fig. 7a show the standard deviation of the data around their group center. These standard deviations are much larger than the distances between the groups, which shows that there is no unique time development of the data, which is expected for a set containing all the data, making a further differentiation necessary.

The situation is quite different in Fig. 7b where the same diagram for the ICRH test series is depicted (note that CV1 and CV2 in Fig. 7b are different from those in Fig. 7a). Here the standard deviations are smaller than the distances between the groups leading to a unique time evolution as expected for similar discharges.

In Fig. 7c some discharges from another ICRH test series were added to the data of Fig. 7b. In this figure the single data points are displayed, the numbers being the group centers. The data from both sets fit rather well together with the exception of one discharge (asterisks) that shows a time evolution lying rather far away from the others. This could not be seen by a visual inspection of the data and thus shows that group analysis can separate discharges that need a closer examination. The reason for the difference in this case was a slightly changed z-position of the probe.

5. Summary

During the operation period in autumn 1995 sniffer probe measurements were taken for more than 800 discharges. As a first result of these measurements we present examinations on the time behavior of the H/D isotope ratio during ICRH test discharges showing an increase though no H was injected. In these discharges the wall loading with deuterium and a saturation after about 7 discharges could be observed. For NBI heated discharges the evolution of rather large amounts of hydrocarbons could be observed that are due to interaction of the neutral beam with the walls occurring for low plasma densities.

Group analysis is shown to be a promising method to handle the large amount of data gained here. It allows to form sets out of these data from which significant mean values can be derived, and the validity of the chosen set formation can be tested.

References

[1] W. Poschenrieder, K. Behringer, H.-St. Bosch, A. Field, A. Kallenbach, M. Kaufmann, K. Krieger, J. Küppers, G. Lieder, D. Naujoks, R. Neu, J. Neuhauser, C. Garcia-Rosales, J. Roth, R. Schneider and the ASDEX Upgrade Team, J. Nucl. Mater. 220–222 (1995) 36.

[2] M. Bessenrodt-Weberpals, O. Gehre, J. Hofmann, H. Murmann, G. Siller and the ASDEX Team, J. Nucl. Mater. 196–198 (1992) 943.

[3] M. Bessenrodt-Weberpals, F. Wagner and the ASDEX Team, Nucl. Fusion 33 (1993) 1205.

[4] G. Cattanei, D.A. Hartmann, J.F. Lyon, D.A. Rasmussen, V. Plyusnin, W7-AS Team and the ICRF Group, 23rd EPS Conf. on Controlled Fusion and Plasma Physics, Kiev (1996), accepted .

[5] W. Poschenrieder, G. Venus and Y.G. Wang et al., 12th EPS Conf. on Controlled Fusion and Plasma Physics, Budapest, Abstract 9F (1985) II-587.

[6] H. Wolff, P. Grigull, W. Poschenrieder, J. Roth, P. Pech and the W7-AS Team, 19th EPS Conf. on Controlled Fusion and Plasma Physics, Innsbruck, Abstract 6–44 (1992) II-1167.

[7] V. Philipps, E. Vietzke and M. Erdweg, 22nd EPS Conf. on Controlled Fusion and Plasma Physics, Innsbruck, CII (1992) 827.

[8] V. Philipps, E. Vietzke and M. Erdweg, J. Nucl. Mater. 162–164 (1989) 550.

[9] H. Renner, W7-AS Team, NBI Group, ICF Group and the ECRH Group, Plasma Phys. Control. Fusion 31 (1989) 1579.

[10] P. Grigull, H.J. Hartfuss, G. Herre, D. Hildebrandt, R. Jaenicke, J. Kisslinger, H. Maassberg, C. Hahn, H. Niedermeyer, P. Pech, H. Renner, H. Ringler, F. Rau, J. Roth, F. Sardei, U. Schneider, F. Wagner, A. Weller, H. Wobig, H. Wolff, the W7-AS Team, the NBI-Team and the ECRH Group, J. Nucl. Mater. 196–198 (1992) 101.

[11] J.W. Krzanowski, Principles of Multivariate Analysis — A Users Perspective (Clarendon, Oxford, 1990).